DISCRETIZATION OF PROGNOSTIC VARIABLES IN THE VERTICAL BY THE SPECTRAL METHOD

Akira Kasahara

National Center for Atmospheric Research*
Box 3000
Boulder, Colorado 80307-3000

and

H.L. Tanaka

Department of Atmospheric Science
University of Missouri–Columbia
Columbia, MO 65211

1. INTRODUCTION

There are two major approaches—finite difference and spectral—to solve numerically atmospheric prediction equations. Historically, the finite difference approach has been most prevalent in discretizing model variables. In recent years, however, the spectral method has been gaining popularity in discretizing model variables in the horizontal direction. In fact, most operational global forecasting models now adopt spherical harmonic expansions to represent the model variables in the horizontal. As far as the discretization of model variables in the horizontal, we now have the freedom of choice in selecting either the finite difference method or the spectral method.

For discretization of model variables in the vertical, our choice is very much limited to the finite difference method. The reason seems to be not because no attempt has been made in the spectral approach, but because very few references are available in the meteorological literature which demonstrate that the spectral method is a viable alternative to the finite difference method in discretizating model variables in the vertical.

There is one exception to this observation. A variant of the spectral method, called the finite element method (FEM) has been successfully applied. In the FEM, grid-point values are represented by the basis functions which are piecewise polynomials spanned only local grid points centered around the grid point in question. Even though the Galerkin approximation is used to derive discretized prediction equations, their appearance is very much like that of finite difference equations. Therefore, the FEM can be considered a variant of the finite difference method.

Following the first formulation by Staniforth and Daley (1977), a finite element vertical discretization scheme has been adopted for baroclinic primitive equations (Staniforth and Daley, 1979). See also Staniforth (1984) for a review. The accuracy of the finite element vertical discretization for a modified version of Staniforth and Daley (1977) is investigated by Béland *et al.* (1983). Also, the related question of the computational stability of the FEM in such a model is examined by Côté *et al.* (1983). These studies noted some difficulties, namely the presence of relatively large phase errors for the gravity wave modes and the appearance of two-grid length vertical computational modes. These shortcomings are said to be eliminated by Béland and Beaudoin (1985) in a revised formulation of the governing equations, particularly in the treatment of the hydrostatic equation. Staniforth (1985) also reviews other recent developments in the application of finite element vertical discretization to prediction models.

Except for the application of FEM, attempts to discretize model variables in the vertical, using more traditional spectral techniques, are very limited. Francis (1972) proposed application of Laguerre polynomials in $\ell n(p/p_s)$, where p is the pressure and p_s the surface pressure. He presented one example in which this application requires a very small time step to ensure a linear computational stability if the explicit time differencing scheme is used. The source of this difficulty is analyzed by Hoskins (1973). Also, Machenhauer and Daley (1972) used Legendre polynomials for spectral representation in a p/p_s coordinate. In this application, they reported a difficulty in obtaining the geopotential values through integration of the hydrostatic equation unless an extra constraint is imposed on the temperature field.

In the application of spectral techniques, the choice of the basis functions is wide open. Bodin (1974) used the empirical orthogonal function (EOF) representation in the vertical to formulate a quasi-geostrophic prediction model. The EOFs are derived by minimizing the root-mean square difference between the data and the functional representation (Obukhov, 1960; Holmström, 1963). The physics of the atmosphere is reflected sta-

*The National Center for Atmospheric Research is sponsored by the National Science Foundation.

tistically in the characteristics of the EOFs. Another choice of the basis functions is the eigensolutions of the vertical structure equation, referred to as the normal modes, which appears in the formulation of nonlinear normal mode initialization (Kasahara, 1982). Gavrilin (1965) formulated a quasi-geostrophic prediction model, in which the vertical discretization uses orthogonal normal mode functions derived from the vertical structure equation for an atmosphere at rest. Simons (1968) describes the formulation of a quasi-geostrophic model along a similar approach, but the horizontal discretization uses spherical harmonic expansions so that the model is spectral in three-dimensions. To the authors' knowledge, however, his model has never been fully tested.

Kasahara and Puri (1981) represented atmospheric data spectrally in three parameters (zonal wavenumber, meridional and vertical modal indices) using three-dimensional normal mode functions (3-D NMFs). The 3-D NMFs are constructed from the eigensolutions of a global primitive equation model and they are orthogonal functions. Kasahara (1984a) presented the formulation of a global spectral model based on the Galerkin approximation with 3-D NMFs as the basis functions. A linearized version of the model formulation is used to investigate the time dependent response of model normal modes to tropical thermal forcing in the atmosphere at rest (Kasahara, 1984b). As a step toward formulation of a nonlinear spectral model using 3-D NMFs, Kasahara and Silva Dias (1986) extended the work of Kasahara (1984b) by considering the effects of a mean zonal flow with meridional and vertical shear. In this model configuration, it is possible to encounter the situation in which barotropic and/or baroclinic instability occurs. In order to avoid the occurrence of this situation, Kasahara and Silva Dias (1986) investigated only the steady response of planetary waves to stationary tropical heating.

Before treating the problem of baroclinic instability over a sphere with 3-D NMF expansions, we shall discuss the feasibility of solving the traditional Charney(1947)–Green (1960) baroclinic instability problem with vertical normal mode expansions. It turns out that the vertical structure equation which appears in the quasi-geostrophic model is identical to that in the primitive equation formulation. Therefore, it is instructive to demonstrate the applicability of vertical normal mode expansion to the quasi-geostrophic model. We are not aware of any earlier publication dealing with the problem of baroclinic instability by using vertical normal mode expansions, though spectral techniques have been used by previous authors. For example, Simons (1969) adopted harmonic functions in the vertical and Boyd (1987) used rational Chebyshev functions defined on a semi-infinite interval for solving baroclinic instability problems.

In Section 2, we present the results of a baroclinic instability problem which is solved by using vertical normal mode expansions. Section 3 summarizes the present work.

2. BAROCLINIC INSTABILITY PROBLEM

2.1 Basic equations

We choose a vertical coordinate $\sigma(\equiv p/p_s$, where p denotes the pressure and p_s the surface pressure, which is treated as a constant) and a horizontal coordinate $\tilde{x}$, directed eastward. Time is denoted by $\tilde{t}$. We consider perturbation motions superimposed on a mean basic zonal flow $\bar{u}(\sigma)$ which are independent of a meridional coordinate.

The well-known equations of quasi-geostrophic flow on a beta-plane are combined into the following potential vorticity equation for dependent variable $\tilde{\psi}$ in the dimensionless form (Kuo, 1973)

$$\left(\frac{\partial}{\partial t}+U\frac{\partial}{\partial x}\right)\left\{\frac{\partial^2\psi}{\partial x^2}+\mathcal{E}\frac{\partial}{\partial\sigma}\left[\frac{\sigma}{S}\frac{\partial\psi}{\partial\sigma}\right]\right\} + \left\{\beta-\mathcal{E}\frac{\partial}{\partial\sigma}\left[\frac{\sigma}{S}\frac{\partial U}{\partial\sigma}\right]\right\}\frac{\partial\psi}{\partial x}=0 \tag{1}$$

which is to be solved subject to the upper and lower boundary conditions in the dimensionless form

$$\frac{\partial\psi}{\partial\sigma}=0 \qquad \text{at } \sigma=\sigma_T, \tag{2a}$$

$$\left(\frac{\partial}{\partial t}+U\frac{\partial}{\partial x}\right)\frac{\partial\psi}{\partial\sigma}+r\frac{\partial\psi}{\partial t}=\frac{dU}{d\sigma}\frac{\partial\psi}{\partial x} \qquad \text{at } \sigma=1. \tag{2b}$$

In deriving the system of dimensionless equations (1) and (2), we use the following notation:

L_* $\equiv$ Representative horizontal scale
H_* $\equiv$ Representative vertical scale in geometrical height
f_0 $=$ $2\Omega\sin\phi_0$
β_0 $=$ $2\Omega\cos\phi_0/a$
ϕ_0 $=$ Latitude of the beta-plane origin, which is chosen here at 45°N
g $\equiv$ Earth's gravity
Ω $\equiv$ Earth's angular speed
a $\equiv$ Earth's radius
t $=$ $2\Omega\tilde{t}$ (scaled time)
x $=$ $\tilde{x}/L_*$ (scaled x-coordinate)
ψ $=$ $\tilde{\psi}/H_*$ (scaled dependent variable)
U $=$ $\bar{u}/(2\Omega L_*)$
β $=$ $L_*\beta_0/(2\Omega)$
$\mathcal{E}$ $=$ $(f_0L_*)^2/(gH_*)$ (Lamb's parameter)
T_* $=$ gH_*/R
R $=$ Specific gas constant of dry air
S $=$ Γ_0/T_* (dimensionless static stability)
Γ_0 $=$ $\kappa T_0/\sigma - dT_0/d\sigma$ (static stability)
T_0 $\equiv$ Basic state temperature as a function of σ
κ $=$ $R/C_p(\equiv 2/7)$
C_p $\equiv$ Specific heat at constant pressure
r $=$ Γ_0/T_0 evaluated at $\sigma=1$.

The boundary conditions (2) are derived from the statements that the perturbation temperature vanishes at the top, σ_T, and the vertical motion $d\psi/dt$ vanishes at the bottom, $\sigma=1$.

2.2 Vertical normal modes

Solutions to (1) under boundary conditions (2) when the zonal mean flow is absent (i.e., $U = 0$) represent the normal modes of the system. In this case, (1) is separable in terms of two equations: one is referred to as the horizontal structure equation and the other as the *vertical structure equation* which is written in the form

$$\frac{d}{d\sigma}\left[\frac{\sigma}{S}\frac{dG}{d\sigma}\right] + \lambda G = 0, \tag{3}$$

where λ is the separation constant and $G(\sigma)$ denotes the vertical structure function. The boundary conditions (2) are now reduced to

$$\frac{dG}{d\sigma} = 0 \qquad \text{at } \sigma = \sigma_T, \tag{4a}$$

$$\frac{dG}{d\sigma} + rG = 0 \qquad \text{at } \sigma = 1. \tag{4b}$$

The differential equation (3) together with the boundary conditions (4) forms a Sturm–Liouville problem which possesses a nontrivial solution only if the parameter λ is assigned one of a set of permissible values (Hildebrand, 1958). For such a value of λ, say $\lambda = \lambda_n$, the conditions of the problem are satisfied by an expression of the form $G = C\ G_n(\sigma)$ where C is a constant. The permissible values of λ are known as its eigenvalues and the corresponding functions $G_n(\sigma)$ as the eigenfunctions or structure functions. Also, we find that two eigenfunctions, G_i and G_j, are orthogonal. In terms of a new independent variable

$$Z = -\ell n\ \sigma, \tag{5}$$

the orthogonality condition, combined by a proper normalization, is expressed by

$$\int_0^{Z_T} G_i G_j e^{-Z} dZ = \delta_{ij}, \tag{6}$$

where $Z_T = -\ell n\ \sigma_T$.

For the basic state temperature profile $T_0(\sigma)$, we choose

$$T_0(\sigma) = (T_s - T_\infty)\ \exp\ (\kappa \ell n \sigma) + T_\infty, \tag{7}$$

where $T_s = T_0(1)$. This temperature distribution is used by Pekeris (1937) and Gavrilin (1965). Fig. 1 shows the temperature profile T_0 as a function of $Z(\equiv -\ell n\sigma)$ by choosing that $T_s = 302.53$ K and $T_\infty = 83.265$ K based on Fulton and Schubert (1980). We see that T_0 is representative of mean tropospheric temperature distribution.

For the temperature profile (7), dimensionless static stability S in (3) is given by

$$S = \eta/\sigma, \tag{8}$$

where

$$\eta = \kappa T_\infty / T_s. \tag{9}$$

The solutions of the system (3) with (4) for the static stability (8) are discussed by Gavrilin (1965) and Fulton and Schubert (1980). The eigenvalue λ_n in (3) can be expressed as

$$\lambda_n = H_s/D_n, \tag{10}$$

where D_n is referred to as the *equivalent height*.

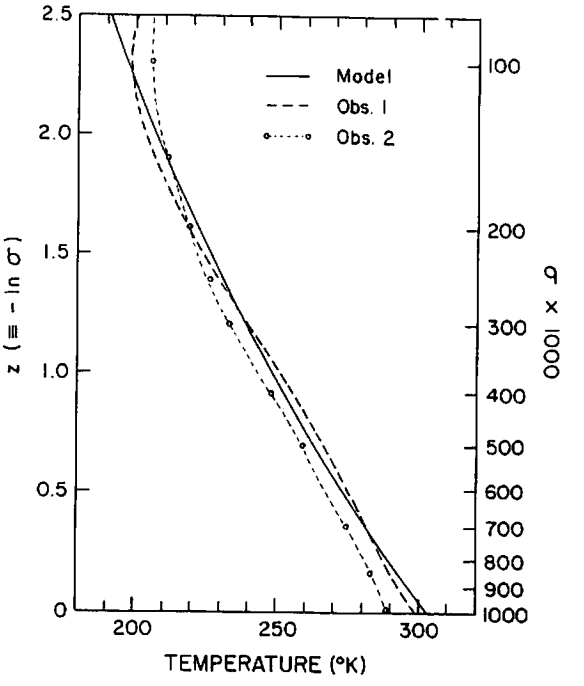

Fig. 1 Model profile of T_0 as a function of $Z(\equiv -\ell n\sigma)$. Obs. 1 denotes a mean tropical temperature distribution (Jordan, 1958) and Obs. 2 a global mean temperature distribution during the FGGE (Tanaka, 1985).

2.2.1 External mode

The mode corresponding to the largest value of D_n is called the *external mode*, indicated by the index $n = 1$. The value of D_1 is obtained by solving the transcendental equation

$$\left(\frac{RT_s}{gD_1} - \frac{1}{2}\right)\ \tanh(\mu\ Z_T) = \mu, \tag{11}$$

where

$$\mu^2 = \frac{1}{4} - \eta\frac{H_s}{D_1} > 0. \tag{12}$$

The eigenfunction G_1 is given by

$$G_1 = A_1\left[\sinh(\mu\ Z) - \frac{\mu}{(0.5 - r)}\cosh(\mu\ Z)\right]\ e^{Z/2}, \tag{13}$$

where

$$A_1 = \left\{\frac{1}{4\mu}\left[1 + \left(\frac{\mu}{0.5 - r}\right)^2\right]\sinh(2\mu Z_T) - 0.5 Z_T\left[1 - \left(\frac{\mu}{0.5 - r}\right)^2\right] + \frac{1}{1 - 2r}\left[1 - \cosh(2\mu Z_T)\right]\right\}^{-\frac{1}{2}}. \tag{14}$$

2.2.2 Internal modes

The modes corresponding to the rest of the eigenvalues are called *internal modes*, indicated by index $n \geq 2$. The values of D_n are obtained by solving

$$\left(\frac{RT_*}{gD_n} - \frac{1}{2}\right) \tan(\xi_n Z_T) = \xi_n, \tag{15}$$

where

$$\xi_n^2 = \eta \frac{H_*}{D_n} - \frac{1}{4} > 0. \tag{16}$$

The eigenfunctions G_n are given by

$$G_n = A_n \left[\sin(\xi_n Z) - \frac{\xi_n}{(0.5-r)} \cos(\xi_n Z)\right] e^{Z/2}, \tag{17}$$

where

$$A_n = \left\{ \frac{-1}{4\xi_n} \left[1 - \left(\frac{\xi_n}{0.5-r}\right)^2\right] \sin(2\xi_n Z_T) + 0.5 Z_T \left[1 + \left(\frac{\xi_n}{0.5-r}\right)^2\right] - \frac{1}{1-2r} [1 - \cos(2\xi_n Z_T)] \right\}^{-\frac{1}{2}} \tag{18}$$

2.2.3 Special case

In solving the vertical structure equation (3) with the boundary conditions (4) for the static stability (8), we assumed that

$$\mu^2 = \frac{1}{4} - \eta\lambda \neq 0. \tag{19}$$

There exists a nontrivial solution for $\frac{1}{4} - \eta\lambda = 0$, if the top Z_T takes the value Z_{TC} defined by

$$Z_{TC} = \frac{4r}{1-2r}. \tag{20}$$

For the temperature distribution (7), the value of r becomes

$$r = \kappa T_\infty / T_* \ (\equiv 0.0786368...) \tag{21}$$

which gives $Z_{TC} = 0.37325...$ (equivalent to $\sigma_T = 0.6885$). Fulton and Schubert (1980) show that for the value of Z_T greater than Z_{TC} there exists a countable number of internal modes in addition to one external mode. We choose that $Z_T > Z_{TC}$.

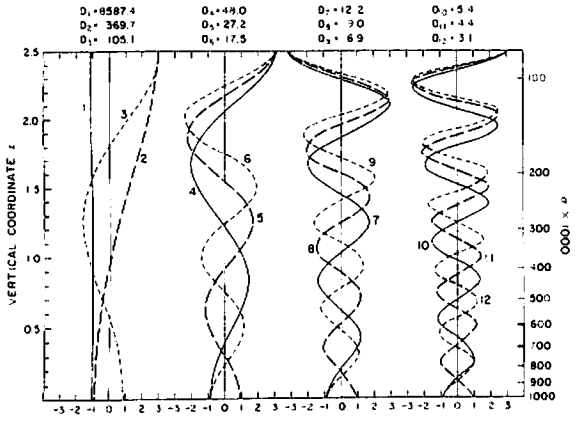

Fig. 2 Vertical profiles of eigenfunctions G_n for the first twelve vertical modes as functions of $Z(\equiv -\ell n\sigma)$. The scale for σ multiplied by 1000 is shown on the right. Numerals besides the profiles indicate modal index n. The values of equivalent height D_n are listed at the top.

2.2.4 Profiles of the vertical structure functions

Figure 2 shows the first twelve vertical profiles of eigenfunctions G_n as functions of $Z(= -\ell n\sigma)$, calculated for the temperature distribution (7) and $Z_T = 2.5$. The values of equivalent height D_n are listed at the top.

2.3 Normal mode expansions

For the basic state temperature distribution (7), the stability parameter S is expressed by (8). We transform the basic equation (1) using the independent variable $Z(\equiv -\ell n\sigma)$. We then assume that

$$\psi = \Psi(Z) \exp\{iK(x - Ct)\}, \tag{22}$$

where K is the dimensionless wavenumber scaled by the length scale L_*^{-1} and C is the dimensionless phase velocity scaled by $2\Omega L_*$. Also, Ψ denotes the amplitude function which depends on Z only.

After the above procedure, the basic equation (1) may be written as

$$(U-C)\left\{K^2\Psi - \frac{\mathcal{E}}{\eta}\left(\frac{d^2\Psi}{dZ^2} - \frac{d\Psi}{dZ}\right)\right\} - \left\{\beta - \left(\frac{d^2U}{dZ^2} - \frac{dU}{dZ}\right)\right\}\Psi = 0 \tag{23}$$

and the corresponding boundary conditions (2) become

$$\frac{d\Psi}{dZ} = 0 \quad \text{at} \quad Z = Z_T, \tag{24a}$$

$$(U-C)\frac{d\Psi}{dZ} + rC\Psi = \frac{dU}{dZ}\Psi \quad \text{at} \quad Z = 0. \tag{24b}$$

In order to determine C in Eq. (23) under the boundary conditions (24), we assume that Ψ and U can be approximated by the following expansions

$$\Psi(Z) = \sum_{n=1}^{N} \frac{1}{\lambda_n} h_n G_n(Z), \tag{25}$$

$$U(Z) = \sum_{n=1}^{N} \alpha_n G_n(Z), \tag{26}$$

where N is an integer and $G_n(Z)$, $N \geq n \geq 1$ are the eigenfunctions of (3) which satisfy the orthogonality condition (6). The coefficient α_n in (26) can be determined for a given distribution of $U(Z)$ by

$$\alpha_n = \int_0^{Z_T} U(Z) G_n e^{-Z} dZ. \tag{27}$$

The vertical distribution of Ψ is obtained once the expansion coefficient h_n in (25) is calculated. It is important to observe that the expansions (25) and (26) permit for Ψ to satisfy the boundary conditions (24), since each $G_n(Z)$ satisfies the boundary conditions (4).

Substituting (25) and (26) into (23), applying the vertical structure equation (3), multiplying the resulting equation by $G_\ell e^{-Z}$, integrating the result with respect to

Z from 0 to Z_T, and utilizing the orthogonality condition (6), we obtain

$$C\left(1+\frac{K^2}{\mathcal{E}\lambda_n}\right)h_n+\beta\frac{1}{\mathcal{E}\lambda_n}h_n - \sum_{k=1}^{N}\left(\sum_{\ell=1}^{N}\alpha_\ell L_{\ell kn}\left[1+\frac{K^2}{\mathcal{E}\lambda_k}-\frac{\lambda_\ell}{\lambda_k}\right]\right)h_k=0, \tag{28}$$

where

$$L_{\ell kn}=\int_0^{Z_T} G_\ell G_k G_n e^{-Z}dZ. \tag{29}$$

Eq. (28) is a system of $N\times N$ linear homogeneous equations. The phase velocity C is determined as an eigenvalue of this system for given values of parameters $\mathcal{E}$, β, and K under a given form of $U(Z)$. The values of interaction coefficient $L_{\ell kn}$ are calculated from the vertical structure functions and the values of λ_n are calculated from the equivalent height. The vector h_n for $n=1$ to N is the eigenfunction corresponding to the phase velocity C. Some of C may appear as complex conjugate pair. In that case, unstable motions are expected from the imaginary part C_i. The phase velocity is calculated from the real part C_r.

2.4 Results

We present results of the stability calculation for a linear basic zonal flow

$$U(Z)=\Lambda Z,$$

where $\Lambda=U_T/Z_T$ with U_T being the basic zonal velocity at $Z=Z_T$. Note that the zonal flow $U(Z)$ in the problem is an approximation to the linear profile, since $U(Z)$ is expressed by a finite number of $G_n(Z)$ as shown by (26).

Fig. 3a shows the growth rate $K|C_i|$ of the gravest unstable mode for resolution $N=9$ as a function of the shear parameter U_T and the wavelength $L(\equiv 2\pi/K)$. The same dimensionless symbols are used in the figure to indicate the units of corresponding dimensional quantities for simplicity. Fig. 3b shows the phase velocity $C-U_M$, where $U_M=U_T/2$. We see the presence of a narrow stable region separating Charney (1947) and Green (1960) types. Note a weak secondary maximum of instability in the Charney type around $L=2000$ km. For $L\leq 1000$ km, it is stable.

Figs. 4a and b illustrate the same as Figs. 3a and b, except for $N=36$. Although the overall patterns are similar, we see differences in detail indicating the dependence of the solutions on resolution N. Actually, Figs. 4a and b resemble to Fig. 6 of Garcia and Norscini (1970) much closer than Figs. 3a and b. For example, now the region for $L\leq 1000$ km appears to be unstable and the narrow stable region separating the Charney and Green types is gone. Also, the growth rate pattern of the Green mode seems to be credible. The dependence of the solutions on vertical modal resolution may be expected as the same problem exists in finite difference solutions dependent on the number of vertical levels (Staley, 1986).

Nevertheless, it is worthwhile to consider the question of convergence in the solutions as modal resolution N increases.

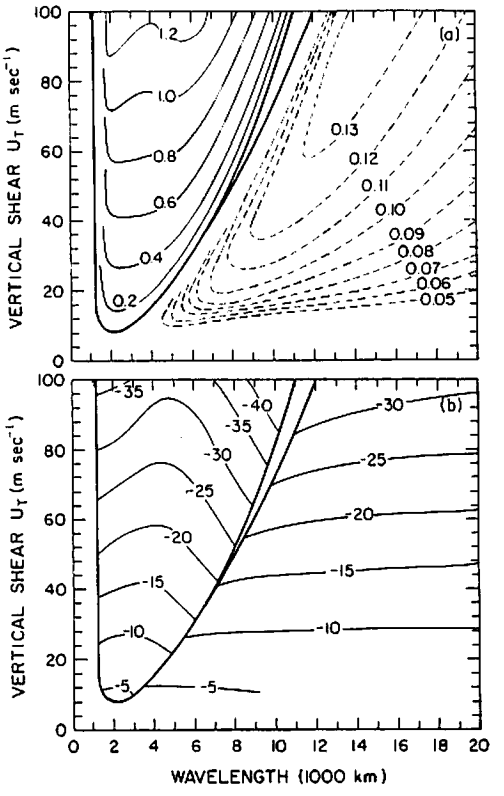

Fig. 3a Growth rate $K|C_i|$ of the gravest unstable mode in units of day^{-1} for modal resolution $N=9$ as a function of vertical shear parameter U_T in m sec^{-1} and wavelength $L(\equiv 2\pi/K)$ in units of 1000 km.

Fig. 3b Same as 3a, except for the phase velocity of the gravest unstable mode, $C-U_M$ in m sec^{-1}, where $U_M=U_T/2$.

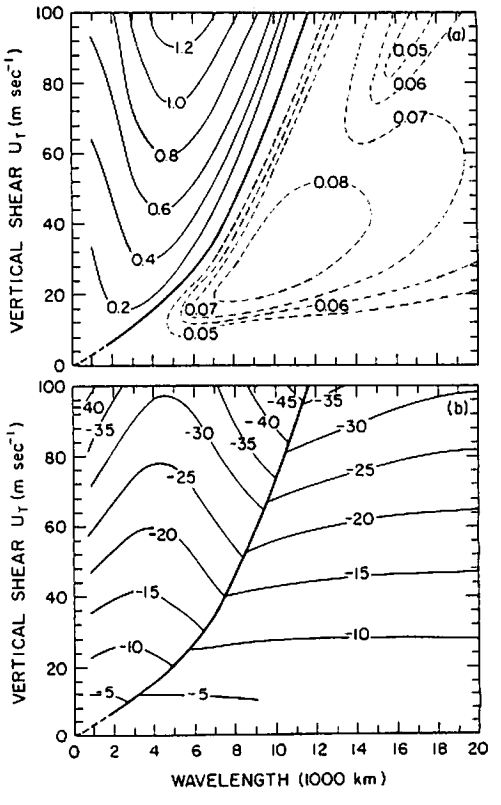

Fig. 4a and 4b are same as Fig. 3a and 3b, respectively, except for modal resolution $N=36$.

Fig. 5a shows the growth rate of the most unstable mode as a function of modal resolution N for the values of U_T corresponding to 100 m sec^{-1} and wavelength L corresponding to 4000 km. Fig. 5b illustrates the same as 5a, except for the phase velocity. It is clear that the numerical solutions undergo a large variation with respect to N, but they quickly approach to a steady state beyond, say $N = 25$. Staley (1986) reported the presence of such a damped oscillation in convergence of solutions with the finite difference method. The value of growth rate for $N = 9$ happens to be very close to the converged value. The case of $N = 36$ is clearly in the state of convergence.

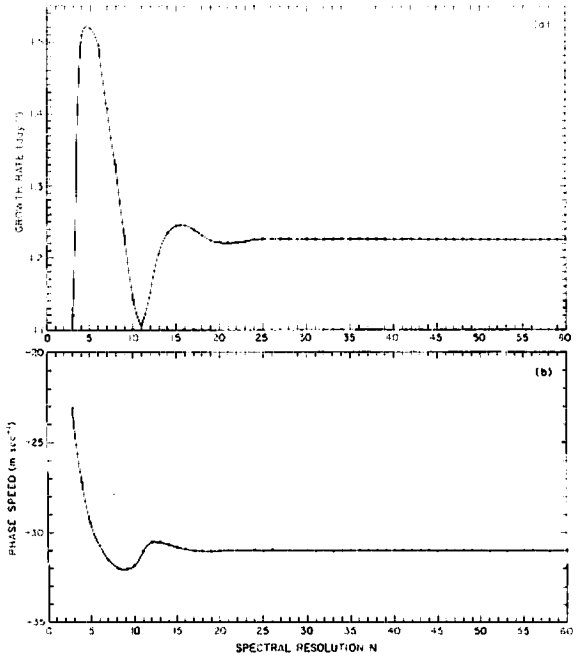

Fig. 5a Growth rate of the most unstable mode as a function of spectral resolution N for U_T=100 m sec^{-1} and $L = 4,000$ km.

Fig. 5b Same as 5a, except for the phase velocity in m sec^{-1}.

Fig. 6 shows the same as Fig. 5, except for the case of L corresponding to 16,000 km. Notice a very different and slow manner of convergence of the solutions in this case, though we can say that the solutions are converging practically beyond, say $N = 50$. Obviously, it is intriguing to ask why solutions of the Green mode are so sensitive to spectral resolution N. We need more research on this question. At least this extreme sensitivity of Green mode on modal resolution may explain the apparent differences in the growth rates of Green modes between Figs. 3a and 4a. Fortunately, the vertical structures of the unstable motions do not appear to depend very strongly on spectral resolution.

Fig. 7 shows the vertical distributions of a normalized amplitude and the phase of ψ for $L = 4,000$ km (upper panel) and $L = 16,000$ km (lower panel) with $U_T = 100$ m sec^{-1}. We show the case of $N = 9$ by solid lines and that of $N = 36$ by dashed lines. Notice that the vertical structures of unstable motions for $N = 9$ and 36 are very close.

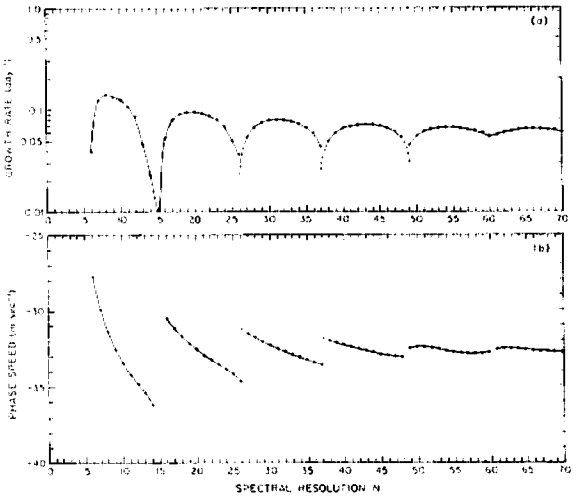

Fig. 6a and 6b illustrate the same as Fig. 5a and 5b, except for $L = 16,000$ km.

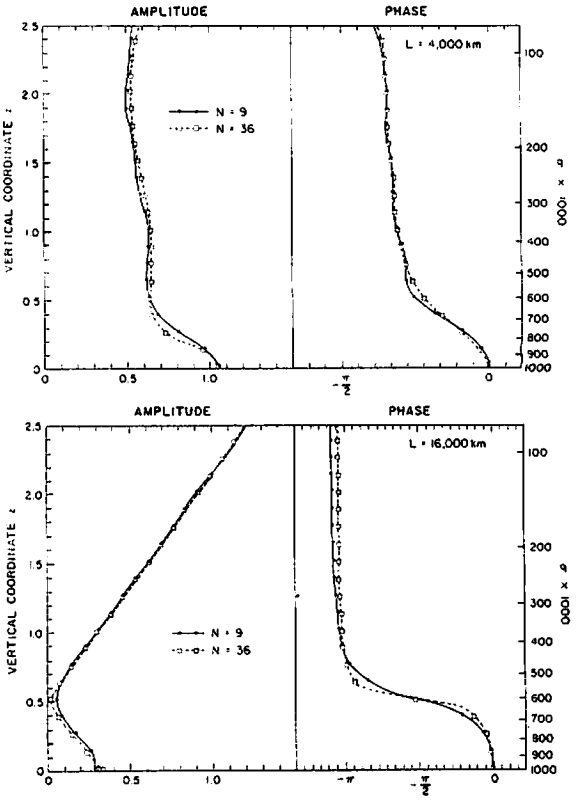

Fig. 7 Upper panel: Vertical distributions of a normalized amplitude and the phase of ψ for $L = 4,000$ km and U_T=100 m sec^{-1}. Lower panel: Same as the upper panel, except for $L = 16,000$ km.

3. SUMMARY

In this paper, we propose to use normal mode functions as the basis functions in the spectral method to discretize model variables in the vertical. As an example, we solve the problem of baroclinic instability of zonal flow in a quasi-geostrophic model using vertical normal mode expansions. The vertical normal modes are constructed as solutions to the vertical structure equation in the case of no zonal flow. The growth rate and phase velocity of unstable motions and their vertical structures are in

agreement with those investigated by Green (1960), Hirota (1968), Garcia and Norscini (1970) and others by using different methods of solution. The sensitivity of the most unstable solutions with respect to the number N of vertical normal mode used is examined in detail. Although the growth rate and phase velocity of most unstable motions indicate the convergence of solutions as N is increased, the manner of convergence exhibits irregular, damped oscillations as in the case of the finite-difference study by Staley (1986). The vertical structures of the most unstable motions appear to be relatively insensitive to the number of vertical mode used. It seems that the normal mode spectral method is a viable alternative to the finite difference method in discretizing model variables in the vertical.

Acknowledgments

Partial support for this research has been provided at NCAR through the National Oceanic and Atmospheric Administration under P.O. No. NA85AAG02575 and at the University of Missouri-Columbia through the National Science Foundation under grant ATM-8410487. The authors wish to thank G. W. Platzman and J. Tribbia for their useful discussions regarding this research. Drafting of the figures was performed by the NCAR Graphics Department and the manuscript was typed by R. Bailey.

References

Béland, M., and C. Beaudoin, 1985: A global spectral model with a finite element formulation for the vertical discretization: adiabatic formulation. *Mon. Wea. Rev.*, **113**, 1910–1919.

——, J. Côté and A. Staniforth, 1983: The accuracy of a finite-element vertical discretization scheme for primitive equation models: comparison with a finite-difference scheme. *Mon. Wea. Rev.*, **111**, 2298–2318.

Bodin, S., 1974: The use of empirical orthogonal functions in quasigeostrophic numerical prediction models. *Tellus*, **26**, 582–593.

Boyd, J. 1987: Orthogonal rational functions on a semi-infinite interval. *J. Comp. Phys.*, **70**, 63–88.

Charney, J. G., 1947: The dynamics of long waves in a baroclinic westerly current. *J. Meteor.*, **4**, 135–163.

Côté, J., M. Béland and A. Staniforth, 1983: Stability of vertical discretization schemes for semi-implicit primitive equation models: theory and application. *Mon. Wea. Rev.*, **111**, 1189–1207.

Francis, P. E., 1972: The possible use of Laguerre polynomials for representing the vertical structure of numerical models of the atmosphere. *Quart. J. Roy. Meteor. Soc.*, **98**, 662–667.

Fulton, S. R. and W. H. Schubert, 1980: Geostrophic adjustment in a stratified atmosphere. Atmos. Sci. Paper No. 326, Dept. Atmospheric Science, Colorado State University, Fort Collins, Co., 80523, 97 pp.

Garcia, R. V. and R. Norscini, 1970: A contribution to the baroclinic instability problem. *Tellus*, **22**, 239–250.

Gavrilin, B. L., 1965: On the description of vertical structure of synoptical processes. *Izv., Atmos. and Oceanic Phys.*, Ser., **1**, 8–17, translated by C. M. Wade.

Green, J. S. A., 1960: A problem in baroclinic stability. *Quart. J. Roy. Meteor. Soc.*, **86**, 237–251.

Hildebrand, F. B., 1958: *Methods of applied mathematics.* Prentice-Hall, 523 pp.

Hirota, I., 1968: On the dynamics of long and ultra-long waves in a baroclinic zonal current. *J. Meteor. Soc. Japan* **46**, 234–249.

Holmström, I., 1963: On a method for parametric representation of the state of the atmosphere. *Tellus*, **15**, 127–149.

Hoskins, B., 1973: Comments on: 'The possible use of Laguerre polynomials for representing the vertical structure of numerical models of the atmosphere' by P. E. Francis. *Quart. J. Roy. Meteor. Soc.*, **99**, 571–572.

Jordan, C. L., 1958: Mean soundings for the West Indies area. *J. Meteor.*, **15**, 91–97.

Kasahara, A., 1982: Nonlinear normal mode initialization and the bounded derivative method. *Rev. Geophys. Space Phys.*, **20**, 385–397.

——, 1984a: Recent mathematical and computational development in numerical weather prediction. *Large Scale Scientific Computation* (Ed. S. Parter), Academic Press, 85–125.

——, 1984b: The linear response of a stratified global atmosphere to tropical thermal forcing. *J. Atmos. Sci.*, **41**, 2217–2237.

——, and K. Puri, 1981: Spectral representation of three-dimensional global data by expansion in normal mode functions. *Mon. Wea. Rev.*, **109**, 37–51.

——, and P. L. da Silva Dias, 1986: Response of planetary waves to stationary tropical heating in a global atmosphere with meridional and vertical shear. *J. Atmos. Sci.*, **43**, 1893–1911.

Kuo, H. L., 1973: Dynamics of quasigeostrophic flows and instability theory. *Advances in Applied Mech.*, **13**, 247–330.

Machenhauer, B. and R. Daley, 1972: *A baroclinic primitive equation model with a spectral representation in three dimensions.* Institute for Theoretical Meteorology, Copenhagen Univ., Denmark, Report No. 4, 63 pp.

Obukhov, A. M., 1960: The statistically orthogonal expansion of empirical functions. *Izv. Geophys. Ser.*, No. 3, 288–291.

Pekeris, C. L., 1937: Atmospheric oscillations. *Proc. Roy. Soc.*, London, A158, 650–671.

Simons, T. J., 1968: A three-dimensional spectral prediction equation. Atmos. Sci. Paper No. 127, Dept. Atmospheric Science, Colorado State University, Fort Collins, Co. 80523, 27 pp.

——, 1969: Baroclinic instability and atmospheric development. Atmos. Sci. Paper No. 150, Dept. Atmospheric Science, Colorado State University, Fort Collins, Co. 80523, 36 pp.

Staley, D. O., 1986: Baroclinic and barotropic instability spectra as functions of N in N-level models. *J. Atmos. Sci.*, **43**, 1817–1832.

Staniforth, A. N., 1984: The application of the finite-element method to meteorological simulations—a review. *Int. J. Num. Meth. Fluids*, **4**, 1–12.

——, 1985: Finite-element modelling-some formulation considerations for atmospheric applications. *GARP Special Report*, No. 43, World Meteorological Organization, Geneva, Switzerland, I. 50–65.

——, and R. W. Daley, 1977: A finite-element formulation for the vertical discretization of sigma-coordinate primitive equation models. *Mon. Wea. Rev.*, **105**, 1108–1118.

——, and ——, 1979: A baroclinic finite-element model for regional forecasting with the primitive equations. *Mon. Wea. Rev.*, **107**, 107–128.

Tanaka, H., 1985: Global energetics analysis by expansion into three-dimensional normal mode functions during the FGGE winter. *J. Meteor. Soc. Japan*, **63**, 180–200.